Prediction Method to Maintain QoS in Weather Impacted Wireless and Satellite Networks

Kamal Harb[1,2], Anand Srinivasan[1], Changcheng Huang[2] and Brian Cheng[1]
1 – EION Wireless, 945 Wellington Street, Ottawa, Ontario, Canada K1Y 2X5
2 – Dept. of Systems and Computer Engineering, Carleton University,
1125 Colonel By Drive, Ottawa, Ontario, Canada K1S 5B6
Email: kharb@sce.carleton.ca

***Abstract*—Rain and snow can have a distorting effect on Ku and Ka bands signal fidelity resulting in excessive digital transmission errors. This loss of signal attenuation is commonly referred to as rain fade. Rain fade impacts the Quality of Service in wireless and satellite networks. A decision support system is therefore necessary for service providers to accurately predict rain fade and establish mitigation planning by adaptively selecting appropriate power level, coding and modulation schemes. This paper establishes an important component of the decision support system by adaptively computing rainfall rate and rain attenuation at any location on earth using ITU-R models combined with bi-linear interpolation and frequency extrapolation. We also introduce a novel method for accurately determining rain attenuation as a function of frequency based on proceeding results from prediction weather database, since rain attenuation is considered a dominant impairment for wireless signals [1]-[6]. Finally, a three dimensional relationship is proposed for rain attenuation with both frequency and probability to provide decision support system with an accurate view of satellite's parameters. The derived parameter values, being fed through neural networks and fuzzy systems to improve estimate Signal to Noise Ratio, will enable the decision support system to maintain Quality of Service and Service Level Agreements by adaptively adjusting satellite signal power, modulation, coding, and data rate at unpredictable weather conditions.**

***Index Terms*—Bit-Error Rate (BER), International Telecommunications Union - Radiocommunications (ITU-R), Quality of Service (QoS), Service Level Agreements (SLA) and Signal to Noise Ratio (SNR).**

I. INTRODUCTION

PROPAGATION impairments affecting Ku and Ka bands satellite links include rain attenuation, gaseous absorption, cloud attenuation, and tropospheric scintillation. Rain attenuation is considered a dominant impairment. Rain attenuation on satellite signals becomes particularly severe at frequencies higher than 10 GHz, especially for small aperture antenna such as Very Small Aperture Terminal (VSAT) and Television Receive Only (TVRO) [3], [5] and [7]. Hence a decision support system is necessary to maintain the QoS and SLAs for a wireless or satellite customer that adaptively adjusts signal power, modulation, coding, and data rate by properly predicting the rainfade.

A number of prediction models are available for the estimation of individual components. However, methodologies that attempt to combine them in a cohesive manner are not widely available [7]-[10]. Furthermore, it is extremely hard to optimally manage satellite-available network resources impacted by rain fade with link traffic engineering only- "Goldilocks Link Budgeting". It is then absolutely necessary to correctly identify and predict the overall impact of every significant rain-attenuating factor on Quality of Service (QoS), be it location, transmission or propagation characteristics along any given path between satellite and ground terminals.

In the absence of detailed knowledge of occurrence probabilities of different impairments, empirical approaches are taken by estimating their combined effects. Once the amounts of expected impairments are established, appropriate methods for mitigating impairments must be invoked. Some of these include up-link power control, adaptive coding, antenna beam shaping, and site diversity [11]-[14].

In view of these analytical approaches, dealing with weather-impacted QoS and reliable satellite communications are currently non-existent. Other thrusts in satellite service providers are shifting their resolution towards intelligent-based computationally efficient prediction methods. These types of methods accurately predict relevant rain metrics, by adaptively applying informed neural and fuzzy systems to regulate (or alter) transmit power, modulation schemes and channel coding. Consequently, the methods will promptly adjust to new signal changes, through the inter-connected network entities, before rain problems actually manifest themselves.

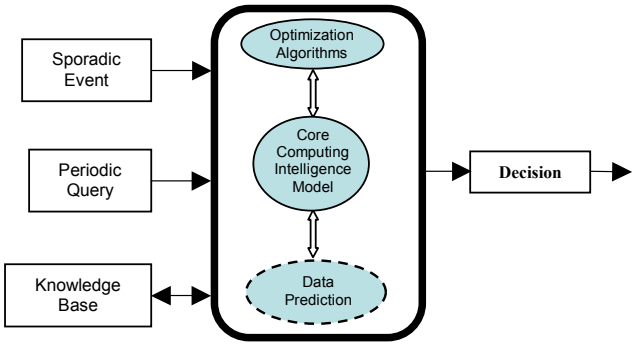

Fig. 1. Network Optimization Decision Support System

Fig. 1 shows the high level architecture of the network optimization decision support system. Rain fade, power, and modulation information are used to obtain optimal decision. The work presented in this paper fits in the data prediction

module and the interface to the core computing intelligence model of the decision support system.

We use ITU-R based models to compute rainfall rate as well as rain attenuation. We introduce a method for accurately determining rain attenuation as a function of frequency based on proceeding results from prediction weather database. Finally, a three dimensional relationship is proposed for rain attenuation with both frequency and probability that provides the decision support system a mechanism to have an accurate view of satellite's parameters. The derived parameters will enable the developed decision support system to maintain QoS and SLAs by adaptively adjusting satellite signal power, modulation, coding, and data rate at unpredictable weather conditions.

The remaining sections of this paper are organized as follows: In section II, we describe the ingredient of DSS, namely existing, approximated and proposed methods along with statistical analysis of rainfall rate, as well as rain attenuation as a function of both frequency and probability at different locations. It is then followed by simulation and analysis of numerical results in section III. Finally, discussion, conclusion and prospective work are outlined in section IV.

II. Theory And Results

Data files collected from ITU-R for *PR*, *MC* and *MS* contain numerical values for the variables: P_R (*Lat, Long*), M_C (*Lat, Long*) and M_S (*Lat, Long*) respectively. These data files represent a weather characteristic model to derive rainfall rate at different *X* (Longitude degree) and *Y* (Latitude degree) on earth. Data files *Lat* and *Long* contain latitude and longitude for each data entry in all files [1], [2] and [4].

II.1 Rainfall Rate Calculation

Rainfall rate is a factor used to determine rain fade. Rain fade seems to correlate very closely with the volume of raindrops along the path of propagation. Therefore, rainfall rate can be computed by:

1) Extracting variables P_R, M_C and M_S for the four points closest in *Lat* and *Long* to the geographical coordinates (*X* and *Y*) of the desired location. Latitude grid ranges {90°N to -90° S}, and longitude grid ranges {0 to 360°} both for 1.5° steps.

a. If the location falls on the grid, we will take these values as is from the given ITU-R tabulated data.

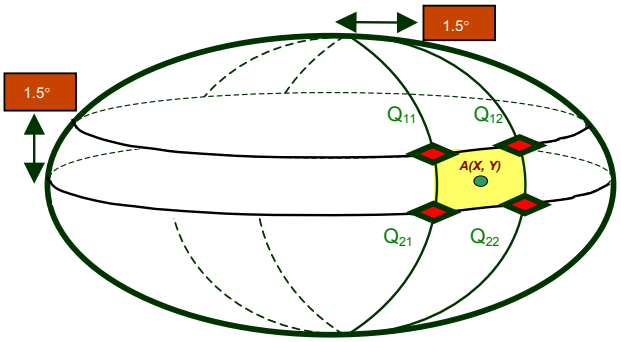

Fig. 2. Grid Point Location

b. If it does not fall on the grid, we perform a bi-Linear interpolation to the four closest grid points as shown in Fig. 2.

2) Deriving percentage probability of rainfall in an average year, P_0, based on calculated data collected from previous steps, where:

$$P_0(Lat,Long) = P_R(Lat,Long)\left(1 - e^{-0.0117(M_S(Lat,Long)/P_R(Lat,Long)}\right). \quad (1)$$

a. If $P_R = 0$, the result of this operation will be undetermined and consequently rainfall intensity will also be zero [1]. In this case we shall stop the procedure.

b. If $P_R \neq 0$, we shall derive rainfall rate, R_p, from exceeded percentage probability of interest *p*, where *p* should be $\leq P_0$, otherwise $P_0 = 0$ and the following steps will not be required.

Where:

$$a = 1.11,\ b = \frac{(M_C(Lat,Long) + M_S(Lat,Long))}{22932P_0} \text{ and } c = 31.5 * b. \quad (2)$$

$$A = a * b, B = a + c * \ln(p / P_0(Lat,Long)) \text{and } C = \ln(p / P_0(Lat,Long)). \quad (3)$$

Thus, rainfall rate will be:

$$R_p(Lat, Long) = \frac{-B + \sqrt{B^2 - 4 * A * C}}{2 * A} \ mm/hr. \quad (4)$$

For example, using (1)-(4), rainfall rate value R_p will be 28.46 mm/hr, for longitude $X = 25$, latitude $Y = 36$, and $p = 0.01\%$. If $P_0 = 0 \Rightarrow R_p$ from (4) will also be zero.

II.2 Rain Attenuation Calculation

II.2.1 Existing Method

This section provides ITU-R estimates for long-term statistics of slant-path rain attenuation for any given location at frequencies up to 55 GHz.

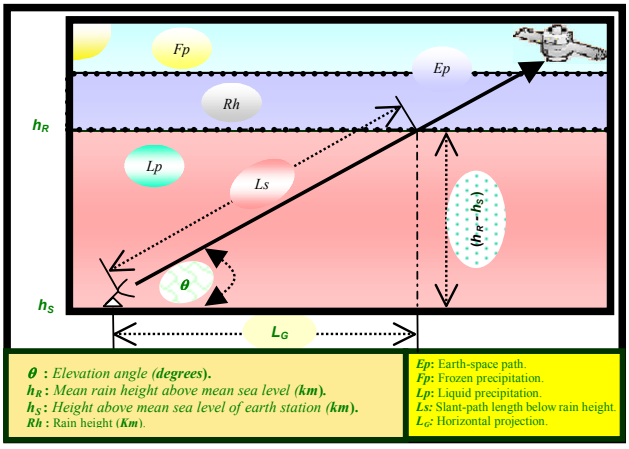

Fig. 3. Earth-Space Path

Fig. 3 shows the relationship of signal propagation parameters. Other required parameters are:

f: Frequency (*GHz*).

ρ: Latitude of earth station (*degrees*).

R_e: Effective radius of Earth (8,500 *km*).

With respect to altitude where rain extends during periods of

precipitation, the following procedure has been recommended:

1) For areas around the world where no specific information is available: The mean 0°C isotherm height above mean sea level h_0 in (*km*) can be obtained from data file *HEIGHT0.txt* (this file may be downloaded from the ITU-R Bureau - BR). Note that data file *HEIGHT0.txt* contains 0°C isotherm height above mean sea level with resolution of 1.5° in both latitude and longitude. The same applies for the grid point data described in the previous section.

2) Mean rain height above mean sea level, h_R, can be obtained from 0°C isotherm h_0 given in [4] as:

$$h_R = h_0 + 0.36 \quad km. \tag{5}$$

3) We shall compute slant-path length, L_S, below rain height from [1], [2], [4] and [6]; the following formulas are used:

i- For $\theta < 5°$: $$L_S = \frac{2(h_R - h_S)}{\left(\sin^2\theta + \frac{2(h_R - h_S)}{R_e}\right)^{1/2} + \sin\theta} \quad km. \tag{6a}$$

ii- For $\theta \geq 5°$: $$L_S = \frac{(h_R - h_S)}{\sin\theta} \quad km. \tag{6b}$$

if $(h_R - h_S) \leq 0$, then predicted rain attenuation for any time percentage = 0 and steps *4-11* are not required.

4) Calculate horizontal projection, L_G, of slant-path length from: $$L_G = L_S \cos\theta \quad km. \tag{7}$$

5) Find rainfall rate, $R_{0.01}$, exceeded for p = 0.01% of an average year. If $R_{0.01}$ = 0, then predicted rain attenuation = 0 for any time percentage and steps *6-11* are not required.

6) Compute specific attenuation, γ_R, using frequency-dependent coefficients as given in [2] for k, α and rainfall rate R_p, calculated in section II.1 for p = 0.01%, determined from (4), by using: $$\gamma_R = K \left(R_{0.01}\right)^{\alpha} \quad dB/km. \tag{8}$$

For linear and circular polarization and for all path geometries, coefficients in (8) can be computed from (9) and (10) as:

$$K = \left[K_H + K_V + (K_H - K_V)\cos^2\theta\cos 2\tau\right]/2. \tag{9}$$

$$\alpha = \left[K_H\alpha_H + K_V\alpha_V + (K_H\alpha_H - K_V\alpha_V)\cos^2\theta\cos 2\tau\right]/2k. \tag{10}$$

where K_H, α_H and K_V, α_V are constants for the coefficients of horizontal and vertical polarizations respectively.

7) Calculate horizontal reduction factor, $r_{0.01}$, for 0.01% of time: $$r_{0.01} = \frac{1}{1 + 0.78\sqrt{\frac{L_G \cdot \gamma_R}{f}} - 0.38\left(1 - e^{-2L_G}\right)}. \tag{11}$$

8) Calculate vertical adjustment factor, $v_{0.01}$, for 0.01% of time: $$\sigma = \tan^{-1}\left(\frac{h_R - h_S}{L_G \cdot r_{0.01}}\right) \quad degrees. \tag{12}$$

For $\sigma > \theta$, the actual slant-path length L_R will be:

$$L_R = \frac{L_G \cdot r_{0.01}}{\cos\theta}; \text{ else } L_R = \frac{(h_R - h_S)}{\sin\theta} \quad km. \tag{13}$$

$$\text{if } |\rho| < 36° \Rightarrow \chi = 36 - |\rho| \text{ ; else } \chi = 0 \quad degrees. \tag{14}$$

$$v_{0.01} = \frac{1}{1 + \sqrt{\sin\theta}\left(31\left(1 - e^{-\left(\theta/(1+\chi)\right)}\right)\frac{\sqrt{L_R \cdot \gamma_R}}{f^2} - 0.45\right)}. \tag{15}$$

9) Effective path length is: $$L_E = L_R \cdot v_{0.01} \quad km. \tag{16}$$

10) Predicted attenuation exceeded for 0.01% of an average year is obtained from: $$A_{0.01} = \gamma_R \cdot L_E \quad dB. \tag{17}$$

11) For other percentages of an average year, estimations of rain attenuation exceeding, ranging from 0.001% to 5%, can be computed from (17) for an average year as follows:

if $p \geq 1\%$ *or* $|\rho| \geq 36° \Rightarrow \beta = 0$,

else if $p \leq 1\%$ *or* $|\rho| < 36°$ *and* $\theta \geq 25° \Rightarrow \beta = -0.005(|\rho| - 36)$,

otherwise $$\beta = -0.005\left(|\rho| - 36\right) + 1.8 - 4.25\sin\theta. \tag{18}$$

$$A_p = A_{0.01}\left(\frac{p}{0.01}\right)^{-(0.655 + 0.033\ln(p) - 0.045\ln(A_{0.01}) - \beta(1-p)\sin\theta)} \quad dB. \tag{19}$$

The above equation was tested by ITU-R and found to be the most accurate overall of all tested models [1]-[6]. This method provides an accurate solution for rain attenuation at any frequency. However, in order to solve rain attenuation problem, we have to go through (5) to (19) for every frequency sample, a process that requires a large computational load. Therefore, to overcome this problem a novel method will be proposed in section *II.2.3*.

II.2.2 Approximated Method

In the previous section, the value of rain attenuation was processed as a function of probability. By using an approximated method as described below, we can compute the rain attenuation behavior for the whole range of applicable frequencies, using (20)-(23), based on a fixed sample frequency (F_i). Thus, rain attenuation as a function of frequency (f) is calculated as follows:

$$\varphi(f_n) = \frac{f_n^2}{1 + 10^{-4} f_n^2}, \tag{20}$$

$$A(F_i) = \gamma_R(F_i) \cdot L_E(F_i) \quad dB. \tag{21}$$

$$H(\varphi(F_i), \varphi(f_n), A(F_i)) = 1.12 \times 10^{-3}\left(\varphi(f_n)/\varphi(F_i)\right)^{0.5}\left(\varphi(F_i)\,A(F_i)\right)^{0.55}. \tag{22}$$

$$A(f_n) = A(F_i)\left(\varphi(f_n)/\varphi(F_i)\right)^{(1 - H(\varphi(F_i),\ \varphi(f_n),\ A(F_i)))}. \tag{23}$$

where $A(f_n)$ is an equiprobable value of excess rain attenuation at any frequency (f).

Therefore, if reliable attenuation data measured at one frequency (F_i) is available (preferably a higher frequency

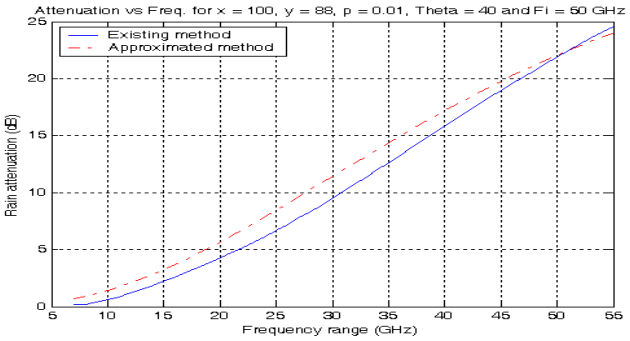

Fig. 4. Existing and Approximated Method Comparison for relatively small R_p

sample since it offers better results for most cases), these empirical formulas will then give rain attenuation as a function of the chosen frequency [6]. Such attenuation can be applied for frequency scaling on the same path ranging from 7 to 55 GHz.

The results will be computed for different specific inputs of prediction of a given percentage of average year probability (p), for different theta angles (θ), for frequency sample (F_i) and for different (X and Y) locations.

However, it is accurate only under a specific condition: when rainfall rate, R_p, is reasonably small (6.277 mm/hr), as shown in Fig. 4. Thus, high frequency sample (F_i) will not guarantee delivering accurate solutions for all models, as we will demonstrate in the following section.

II.2.3 Proposed method

In order to overcome problems associated with inaccuracies and CPU inefficiencies for estimating rain attenuation at different locations, we propose a novel method to maintain and improve QoS by perfectly matching the existing accurate results up to higher frequencies by solving (24) at any single frequency ranging from 7 to 55 GHz and deriving all other attenuations at any other frequency within the same range recursively merely out of (24)-(26).

In this section, we will inspect this method and associate its results to sections II.2.1 and II.2.2. We shall also attempt to find a solution for the presented problem.

In order to achieve reasonable results, we will make sure that the proposed method will give accurate solutions compared to the approximate one, and will improve CPU time.

Earlier, the approximated method was done according to value of rain attenuation calculated at a specific frequency (F_i). By following the empirical formulas (21)-(23), we were able to extrapolate values of rain attenuation at any frequency ranging from 7 to 55 GHz based on calculated rain attenuation at (F_i)**.**

Equations (24)-(26) compute rain attenuation as a function of any frequency (f). Fig. 5 shows a comparison between the existing, approximated and proposed methods. The latter being the new technique presented as:

$$A(f_n) = \gamma_R(f_n) \cdot L_E(f_n)\, dB. \quad (24)$$

Also, any specific frequency ranging from 7 and 55 GHz is obtained from:

$$H(\varphi(f_{n-1}),\varphi(f_n),A(f_{n-1})) = 1.12\times10^{-3}\left(\varphi(f_n)/\varphi(f_{n-1})\right)^{0.5}(\varphi(f_{n-1})A(f_{n-1}))^{0.55}. \quad (25)$$

$$A(f_n) = A(f_{n-1})\left(\varphi(f_n)/\varphi(f_{n-1})\right)^{(1-H(\varphi(f_{n-1}),\,\varphi(f_n),A_1(f_{n-1})))}\, dB. \quad (26)$$

where $\boldsymbol{A}(f_{n-1})$ and $\boldsymbol{A}(f_n)$ are equiprobable values of excess rain attenuation at frequency (f_{n-1}) and (f_n), respectively.

Methods explained so far, are used to investigate the dependence of rain attenuation statistics on elevation angle, polarization, rainfall rate, probability and frequency. These are therefore useful general tools for scaling rain attenuation according to these parameters. Thus, if reliable attenuation data measured at any specific frequency is available, the previous empirical formulas shown in (24)-(26) will then provide rain attenuation as a function of preceding frequency. Rain attenuation can be applied for frequency scaling on the same path ranging from 7 to 55 GHz.

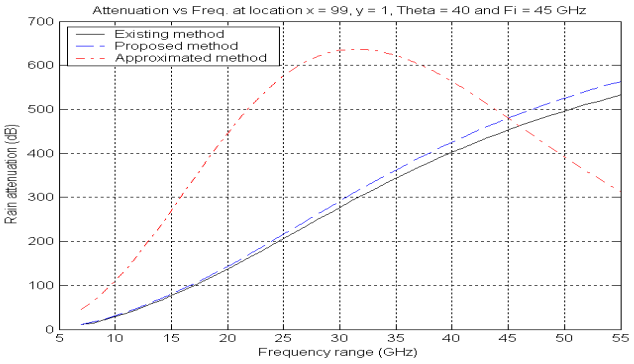

Fig. 5. Existing, Proposed and Approximated Method Comparison for relatively high R_p

Thus, the technique mentioned in section II.2.2 is not accurate for most cases especially when we deal with relatively high rainfall rate (R_p = 120.19 mm/hr) even when applying high frequency sample (F_i = 45 GHz) as in Fig. 5.

This new technique is based on getting results of next frequencies out of preceding ones. This means once we have rain attenuation at any frequency ranging from 7 to 55 GHz, we can then compute rain attenuation for upper frequency on the same path based on prior frequency and so on until we reach the maximum desired frequency. Therefore, it provides high CPU efficiency, since we do not have to repeat the entire calculation from the beginning for each frequency, as is the case for existing solution.

III. SIMULATION RESULTS

In this section we propose new results for rain attenuation as a function of both frequency (f) and probability (p) by combining several computer programs. Thus, (27)-(29) show an appropriate technique for calculation of rain attenuation for different frequencies ranging from 7 to 55 GHz, and for different probabilities ranging from 0.001% to 5%.

The predicted attenuation of an average year for different frequencies and different probabilities can be obtained from:

$$A(f, p) = \gamma_R(f, p) \cdot L_E(f, p)\, dB. \quad (27)$$

Notice that $\boldsymbol{A}$ is a function of both frequency (f) and probability (p).

$$H(\varphi(f_1),\varphi(f_2),A(f_1,p_1)) = 1.12\times10^{-3}\left(\varphi(f_2)/\varphi(f_1)\right)^{0.5}(\varphi(f_1)A(f_1,p_1))^{0.55}. \quad (28)$$

$$A(f_2,p_2) = A(f_1,p_1)\left(\varphi(f_2)/\varphi(f_1)\right)^{(1-H(\varphi(f_1),\varphi(f_2),A(f_1,p_1)))}\, dB. \quad (29)$$

where $\boldsymbol{A}(f_1, p_1)$ and $\boldsymbol{A}(f_2, p_2)$ are equiprobable values of excess rain attenuation at any frequency (f) and any probability (p), respectively.

This model helps and provides the designer with a perceptible view of approximate rain attenuation values that can be computed at any desired location (X and Y), for all range of operational frequencies, percentages for the average

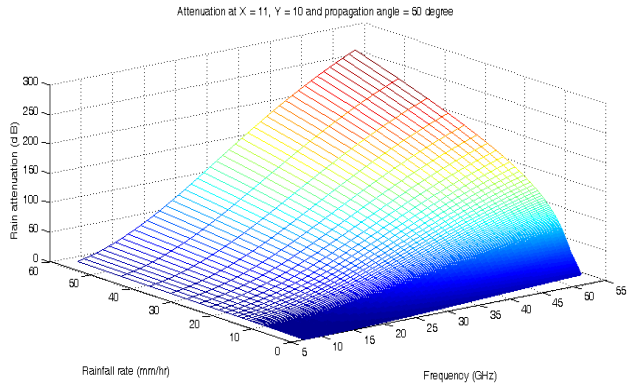

Fig. 6. Rain Attenuation – Function of Frequency and Probability

year probability (p) prediction, and for any angle theta (θ) as shown in Fig. 6.

Therefore, knowing this data will be an immense asset to support analysis for determining the desired operational parameters for the satellite systems around the world.

IV. Conclusion And Future Works

Signal fading caused by rain, limits service quality of satellite links and system availability that operate at frequencies above Ku-band. In most situations, satellite links that operate at such frequencies are designed to be up-link limited. Up-link power control is one of the most cost-effective rain fade mitigation techniques. It enhances link availability and performance.

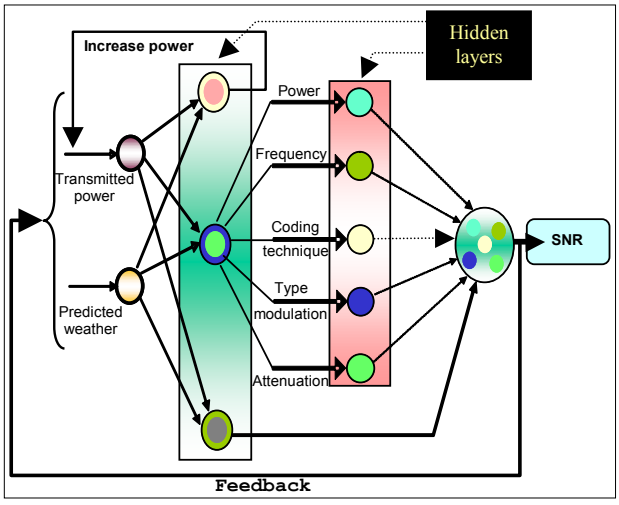

Fig. 7. Proposed method using fuzzy and neural network technique

Rain attenuation is a function of frequency, probability, elevation angle, polarization angle, rain intensity, raindrop size distribution and raindrop temperature. Therefore, it is the dominant propagation impairment when facing high frequency. The proposed method improves QoS by providing accurate results for rain attenuation in lieu of a wide range of frequencies and probabilities combined together. This periodically-computed attenuation will keep updating our knowledge input to our Decision Support System (DSS).

For future research activities, we will use our proposed method to build up a flexible and intelligent system based on neuro-fuzzy systems – Optimized Algorithms and Core Computing Intelligence Model (DSS) – that would be controlled by predicted weather knowledge. Such system will proficiently search for different combinations of input control variables such as transmit power level, modulation schemes and channel coding rates etc. to minimize estimated rain attenuation effect and maximize channel robustness and efficiency by improving SNR as shown in Fig. 7.

Real-time channel measurements such as Signal Noise Ratio (SNR) and Bit Error Rate (BER) can also serve as feedback tuning control to our DSS and adaptively modifying input control variables for clear channel optimization if required.

The main objective, of our upcoming results, is to improve SNR and to solve the rain fade problem due to bad weather conditions at any location.

Acknowledgments

The authors wish to thank:
- Bharat Rudra of OCE and Derek Best of Precarn for supporting this project,
- Andre Bigras and Abdul Lakhani of Telesat for verifying the applicability and usefulness for satellite systems,
- Kalai Kalaichelvan and Rama Munikoti of EION for supporting this research.

References

[1] ITU-R, "Characteristics of precipitation for propagation modeling", Recommendation ITU-R P.837-4, 2001, P. Series Fascicle, Radio wave propagation, International Telecommunication Union, Geneva.

[2] ITU-R, "Specific attenuation model for rain for use in prediction methods", Recommendation ITU-R P. 838-3, 2003, P. Series Fascicle, Radio wave propagation, International Telecommunication Union.

[3] R. K. Crane, "Prediction of the Effects of Rain on Satellite Communication Systems", Proc. of the IEEE, Vol. 65, No.3, pp. 456-474, March 1977.

[4] ITU-R, "Rain height model for prediction methods", Recommendation ITU-R P.839-3, 2001, P. Series Fascicle, Radio wave propagation, International Telecommunication Union, Geneva.

[5] A. Dissanayake, J. Allnutt, F. Haidara, "A prediction model that combines rain attenuation and other propagation impairments along Earth-satellite paths", IEEE Trans. on Antennas & Propagation, Volume 45, Issue 10, pp. 1546 – 1558, Oct. 1997.

[6] ITU-R, "Propagation data and prediction method required for the design of Earth-space Telecommunication systems", Recommendation ITU-R P.618-7, 2001, P. Series Fascicle, Radio wave propagation, International Telecommunication Union, Geneva.

[7] T. Boonchuk, N. Hemmakorn, P. Supnithi, M. Iida, K. Tanaka, K. Igarashi, Y. Moriya, " Rain Attenuation of Satellite link in Ku-band at Bangkok ", Information, Communications and Signal Processing, Fifth International Conference, pp. 1093 – 1096, Dec. 2005.

[8] K. Yasukawa, M. Yamada, Y. Karasawa, " Tropospheric scintillation in the 14/11-GHz bands on Earth-space paths with low elevation angles ", IEEE Trans. on Antennas & Propagation, Vol. 36, No. 4, pp. 563 - 569, April 1988.

[9] Garcia-Lopez, J.A. et al, (1988), " Simple Rain Attenuation Prediction Method for Satellite Radio Links," IEEE Trans. on Antennas & Propagation, Vol. 36, No. 3, March 1988.
[10] W. J. Vogel, J. Goldhirsh, " Multipath fading at L band for low elevation angle, land mobile satellite scenarios ", IEEE selected areas in communications, Vol. 13, No. 2, pp. 197 – 204, Feb. 1995.
[11] Ippolito, Louis J., & Thomas A. Russell (1993), "Propagation Considerations for Emerging Satellite Communications Applications," Proc. of the IEEE, Vol. 81, No. 6, pp. 923-929, June 1993.
[12] Karasawa, Y.T., & T. Matsudo, " Characteristics of fading on low-elevation angle Earth-space paths with concurrent rain attenuation and scintillation, " IEEE Trans. on Antennas & Propagation, Vol. 39, No. 5, pp. 657 – 661, May 1991.
[13] A. A. Aboudebra, K. Tanaka, T. Wakabayashi, S. Yamamoto, H. Wakana, " Signal fading in land-mobile satellite communication systems: statistical characteristics of data measured in Japan using ETS-VI ", IEEE Trans. on Microwave, Antennas & Propagation, Vol. 146, No. 5, pp. 349 – 354, Oct. 1999.
[14] A. S afaai-Jazi, H. Ajaz, W. L. Stutzman, " Empirical models for rain fade time on Ku- and Ka-band satellite links ", IEEE Trans. on Antennas & Propagation, Vol. 43, No. 12, pp. 1411 – 1415, Dec. 1995.